Monitoring of an Ancient Landslide Phenomenon by GBSAR Technique in the Maierato Town (Calabria, Italy)

12

Giovanni Nico, Luigi Borrelli, Andrea Di Pasquale, Loredana Antronico, and Giovanni Gullà

Abstract

The work deals the monitoring of a single ancient landslide detected in the Vonace area, southwards of Maierato (Calabria, Italy). A 18-hour-measurement campaign has been carried out using the Ground-based Synthetic Aperture Radar (GBSAR) interferometry technique carried between March, 25th and 26th. Displacement maps have been geolocated and overlaid to a Digital Elevation Model of the scene. It has been observed that the Vonace area is almost stable except two portions located at the foot of the ancient landslide and at the centre of the town, respectively. In both cases, a maximum displacement of about 0.5 mm has been measured. A further campaign is needed to confirm this displacement.

Keywords

Landslide • Ancient block-slide • Monitoring • Radar interferometry • Ground-based synthetic aperture radar (GBSAR)

12.1 Introduction

In this paper we present the first results of an application of a radar interferometry technique for the monitoring of an ancient landslide detected in the Vonace area, southwards of Maierato (Calabria, Italy). The experiment aims to get information useful to plan the monitoring of movements of the ancient block-slide that could be activated concurrently to the Maierato landslide in February 15, 2010 (Borrelli et al. 2014), and then not immediately identifiable by field surveys (geomorfological elements and damage level in buildings). A first campaign of about 18 h has been carried out to study the scene in a short time interval and to set the zero-measurement for future campaigns. The structure of the paper is as follows. The geological and geomorphological properties of the study area are reported in Sect. 12.2. The Ground-Based Synthetic Aperture Radar (GBSAR) interferometry technique is described in Sect. 12.3. Results are presented and commented in Sect. 12.4.

12.2 Geological and Geomorphological Framework

The geology of the study area consists of silicoclastic-carbonate sediments unconformable lying on the ercinian crystalline basement. Miocene transgressive sequence generally starts with gray fossiliferous sandstones of Tortonian age, which gradually evolving upwards to poorly cemented sandstones. The visible thickness of the sandstone unit is about 40 m. Along the Scotrapiti T., with an abrupt contact, the overlying unit is made of Upper Tortonian/Early Messinian age hemipelagic marls. The total estimated

G. Nico (✉)
Consiglio Nazionale Delle Ricerche, Istituto Per Le Applicazioni Del Calcolo, Via Amendola 122/D, 70126, Bari, Italy
e-mail: g.nico@ba.iac.cnr.it

L. Borrelli · L. Antronico · G. Gullà
Consiglio Nazionale Delle Ricerche, Istituto Di Ricerca Per La Protezione Idrogeologica, Via Cavour 4/6, 87036, Rende, Italy
e-mail: giovanni.gulla@irpi.cnr.it

A. Di Pasquale
DIAN Srl, Z.I. La Martella, III Trav.G.B. Pirelli Sn, 75100, Matera, Italy
e-mail: a.dipasquale@dianalysis.eu

G. Lollino et al. (eds.), *Engineering Geology for Society and Territory – Volume 2*,
DOI: 10.1007/978-3-319-09057-3_12,

outcropping thickness ranges from 5 to 15 m. In the surrounding areas of Maierato town the marls pass, upward and through a discontinuity, to Messinian evaporitic limestone made of highly porous, weak, fine grained calcareous banks, interbedded with a decimetric laminated marls. The visible thickness of the unit is about 40 m. The Miocene sequence is closed by silty-clays and silts layers (lower-middle Pliocene) and Pleistocene continental deposits. From a geomorphological point of view in the hamlet of Vonace some morphological elements have been found which could be ascribed to the presence of an ancient block-slide. In particular, aerial-photointerpretation had shown the presence of an ancient block slide in apparent continuity with the Maierato landslide, even if it seems at a more advanced stage of evolution. The boundaries of the block-slide are unclear as a result of the partial obliteration of their morphological evidence due to the presence of a residential area (Fig. 12.1).

Surveys on the field have collected elements confirming this hypothesis. In fact, despite the partial covering of field evidence due to the presence of the inhabited area and of colluvial covers, geological and geomorphological data indicate that in the past the limestone block, at present located in the lower part of the slope, had moved over the underlying hemiphelagic marls. In addition, field evidence

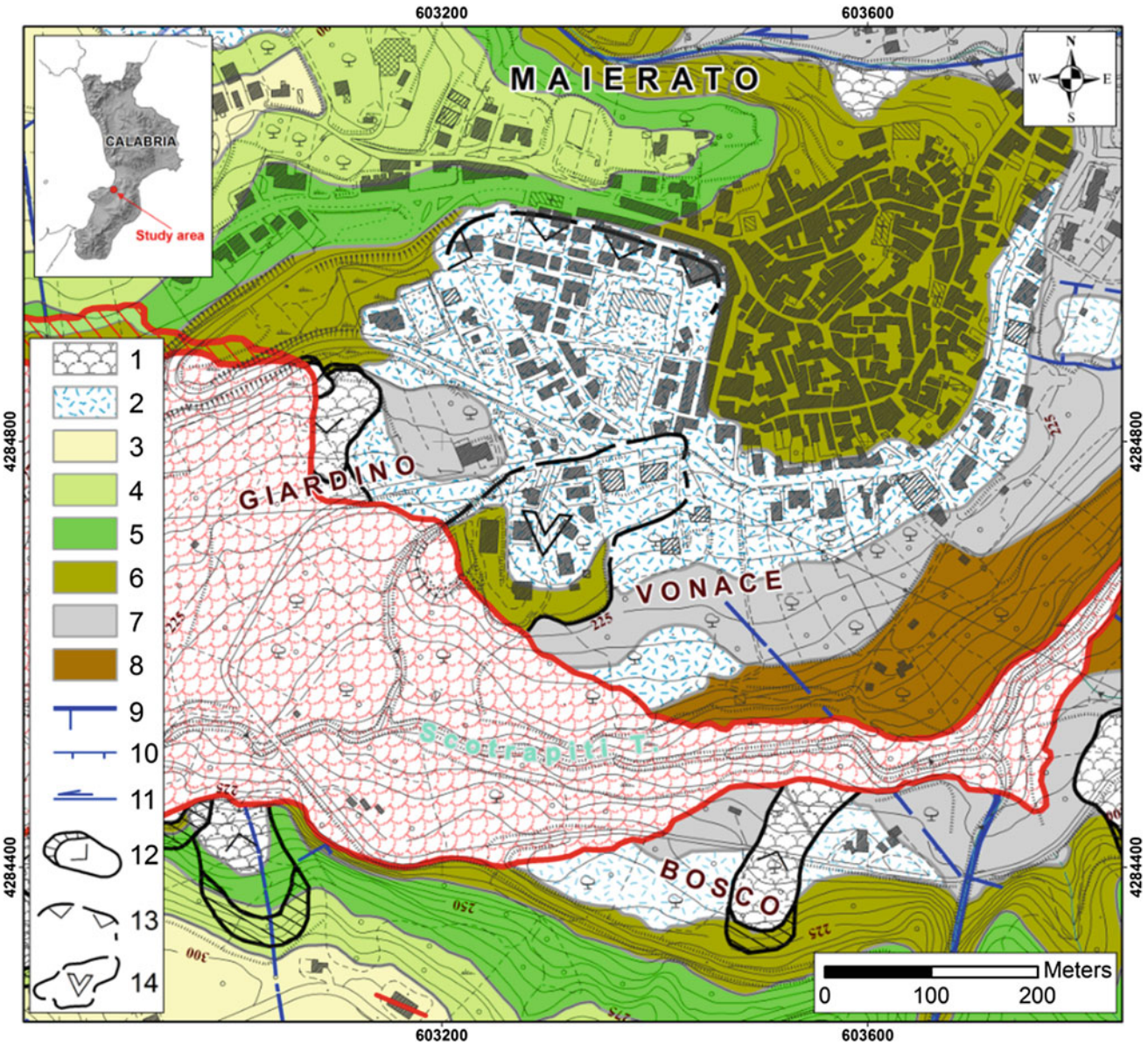

Fig. 12.1 Geological and geomorphological map of the study area. *Legend*: *1* landslide debris; *2* colluvial soils (Holocene); *3* conglomerates and sands (*Middle* Pleistocene); *4* siltly sands (*Middle-Upper* Pliocene); *5* silty clays (*Lower* Pliocene); *6* evaporitic limestones (Messinian); *7* hemipelagic marls (*Upper* Tortonian/Early Messinian); *8* fossiliferous sandstones (Tortonian); *9* major normal fault; *10* secondary normal fault; *11* transcurrent fault; *12* dormant sliding; *13* ancient landslide scarp; *14* ancient block-slide with uncertain boundary

indicate that the limestone block is intensively pervasively jointed and shows a limited back slope tilt. Moreover, a decimetric laminated marl layer, found inside the limestone, shows deformations. Geological and geomorphological evidence indicate that the ancient Vonace block slide is stable under present conditions.

12.3 Ground-Based Synthetic Aperture Radar (GBSAR) Interferometry

A Synthetic Aperture Radar (SAR) is an active microwave sensor used to produce 2D microwave images of the observed scene without the need of solar illumination and in any weather condition. In the last few year, ground-based SAR systems have been developed to solve the problem of continuous monitoring of small scenes, such as dams, landslides, buildings, bridges, or to extract information on terrain morphology (Leva et al. 2003; Di Pasquale et al. 2013; Nico et al. 2005). A ground-based SAR consists of a couple of TX/RX antennas mounted on a computer-controlled positioner that synthesizes a 2 m-long synthetic aperture along the so called azimuth direction. A microwave source illuminates he observed scene at different discrete frequencies within the frequency band 16.70–16.78 GHz. The working range distance to the study area ranges from about less than 50 m up to more than 2000 m. The spatial resolution in range is $\Delta R = 0.75$ m while that in azimuth Δx is given by

$$\Delta x = \frac{\lambda R}{2L} \tag{1}$$

where λ the radar wavelength, R the range distance and L the synthetic aperture. Microwave echoes acquired by radar antennas along the rail are processed to generate a GBSAR complex-valued image. Amplitude is related to the scattering properties of the scene while the phase depends on its geometry and displacements. Figure 12.2 displays on the left an example of amplitude image. It is represented in radar polar coordinates (R,ψ) (see Fig. 12.3) and refers to the Maierato town. The radar amplitude has been normalized to the maximum value and represented in decibels. Besides the antenna's coupling at the near-range, yellow pixels corresponds to buildings or similar natural or man-made structures giving the higher backscattering response to the radar signal. Objects in the scene are separated by distances and not angles as in common optical images. Usually, amplitude images are used to identify objects in the scene directly in the field since the bigger structures gives the stronger radar response. In interferometric applications a GBSAR system acquires a time series $\{S_i, i = 1,\ldots N\}$ of coherent SAR images of the scene with a minimum sampling period of 5 min. For each pair of SAR images acquired in an interferometric configuration, an interferometric phase image is computed as follows

$$\Delta\varphi = \arctan\{S_1 \cdot conj(S_2)\} \tag{2}$$

where $S1 = |S1|\exp(i\varphi 1)$ and $S2 = |S2|\exp(i\varphi 2)$ are the two coherent SAR images acquired at times t_1 and t_2. The properties of inteferometric coherence depends on the spatial and temporal stability of the scattering properties of the scene and is estimated as the real-valued $\gamma \in [0, 1]$ given by

$$\gamma = \frac{|S_1 \cdot conj(S_2)|}{\sqrt{|S_1|^2 \cdot |S_2|^2}} \tag{3}$$

Figure 12.2 displays on the right an example of coherence map corresponding to Maierato town. The coherence depends on both the properties of the observed scene and the

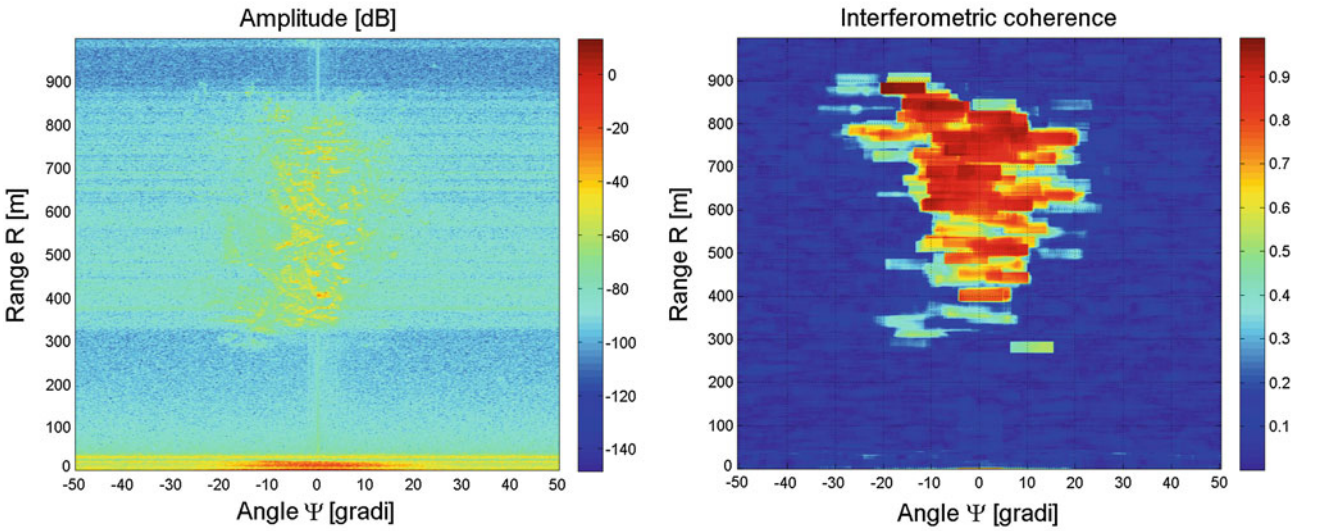

Fig. 12.2 Amplitude (*left*) and coherence (*right*) image of the Maierato scene

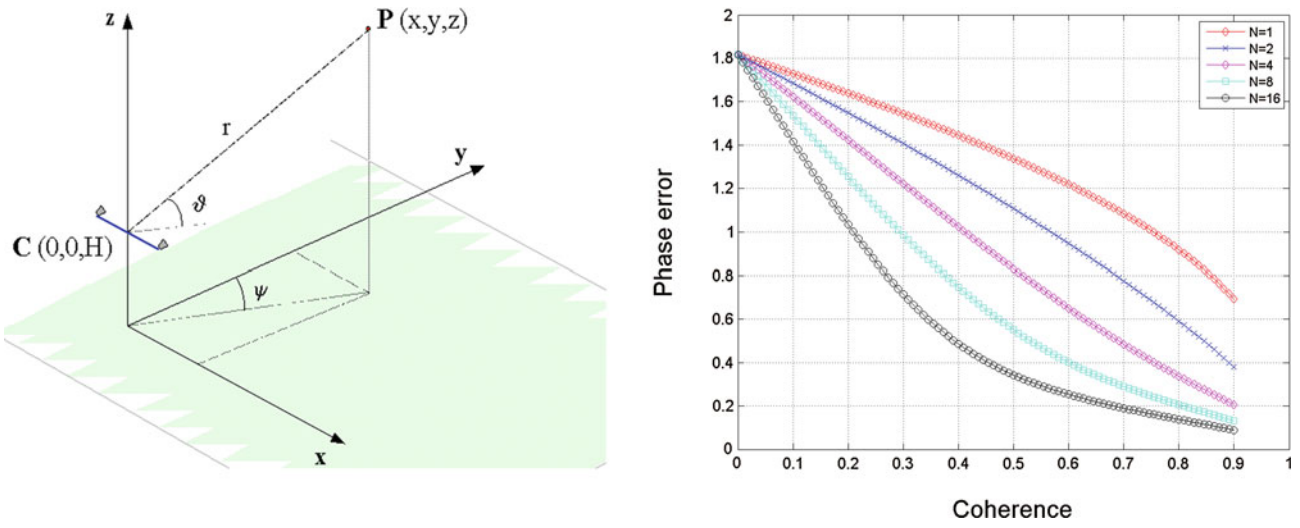

Fig. 12.3 Reference system of GBSAR images (*left*) and phase precision vs interferometric coherence. Different dimensions are used for the low-pass filter kernel (*right*)

acquisition configuration. Man-made structures have high coherence values while areas covered by a huge vegetation gives rise to coherence losses due to random movements of leaves and branches. Besides the scene properties, also the capability to re-install the GBSAR system at the same position with an accuracy of a few millimetres can also affect interferometric coherence. A way to solve this problem consists in constructing a temporary fixed structure in front of the monitored scene, easily removable if needed, so as to accurately re-positioning the GBSAR rail. The most important application of GBSAR interferometry is the measuring of displacements of a whole area. The displacement D of a point P (see Fig. 12.3) in the scene is related to the interferometric phase Δφ by the relationship

$$D = \frac{\lambda}{4\pi}\Delta\varphi \tag{4}$$

where λ is the radar wavelength that for the radar used in this work is λ = 18 mm. As can be observed in Eq. (4), the precision of displacement measurements depends only on the accuracy of phase measurements. The relationship between the phase precision and the interferometric coherence is reported in Fig. 12.2. The relationship depends on the low-pass filter kernel dimension used to reduce phase noise.

12.4 Results

The GBSAR acquired a time series of 203 SAR images at time intervals of about 7 min. An example of SAR images amplitude acquired in this campaign is shown in Fig. 12.2. The quality of the interferometric signal acquired over the Maierato scene is given by the coherence map displayed in Fig. 12.2. Both the amplitude and coherence images are used to derive a mask to overlay over the displacement map in order to remove area with a low signal-to-noise ratio. Figure 12.4 shows the map of total displacement measured by GBSAR interferometry during the 17 h-campaign, between march 25th, 3:00 pm and march 26th, 8:00 am. Displacement are referred to the radar's line-of-sight direction and represented in the coordinate system of Fig. 12.3. Positive and negative displacements represent, respectively, a movement away from and toward the radar. The map shows a stability of the area within the time interval of data acquisition. The spatial distribution of displacement values can be explained in terms of the precision of GBSAR interferometry (see Fig. 12.3 and Eq. (4). For coherence values greater than 0.4, the displacement map filtered with a low-pass filter kernel N = 5, has an expected precision of less than 1 mm. The corresponding geolocated map is displayed in Fig. 12.4. Displacement values in the geolocated map have been also classified in three groups: (a) values in the range [−0.5, 0.5] mm, basically corresponding to stable areas, (b) values smaller than −0.5 mm, (c) values higher than 0.5 mm. The area belonging to the groups (b) and (c) could correspond to displacements, respectively, toward and away from the radar position. Even if all measured displacement values can be explained in part in terms of measurement precision, values belonging to groups (b) and (c) could be consistent with slow movements. Useful information about these possible slow movements would be provided by a monitoring campaign that must consider: temporal coverage (about 1–2 years), temporal baseline

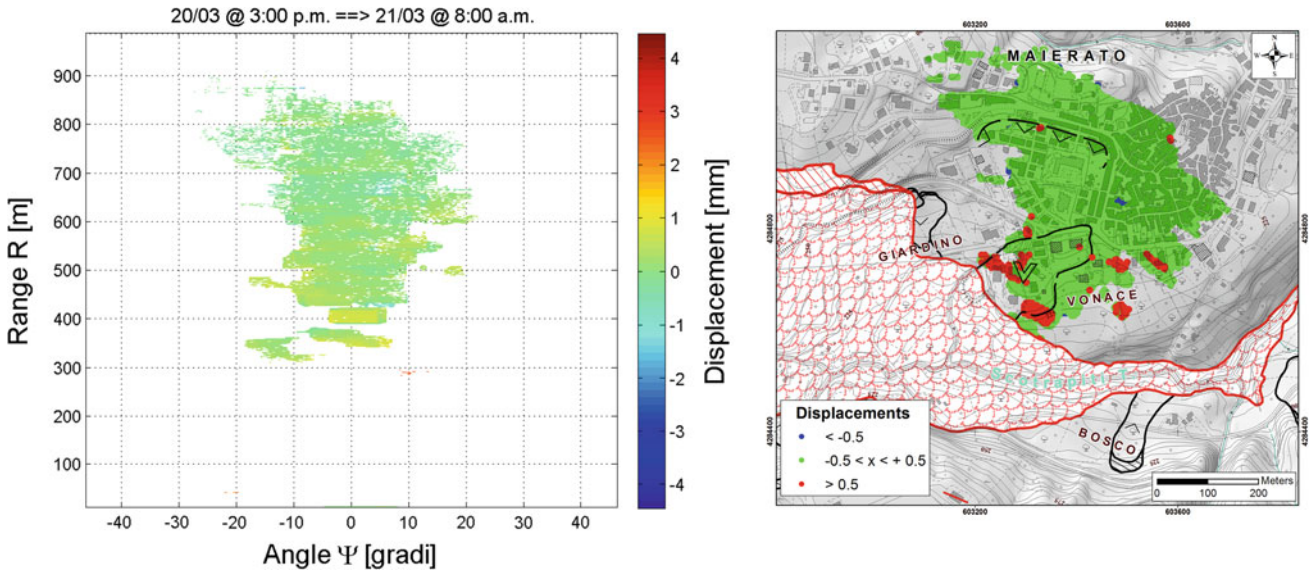

Fig. 12.4 Map of displacements measured by GBSAR over the Maierato scene in radar coordinates (*left*), geolocated and overlaid to landslide mapping (*right*)

between campaigns (about 3 months), view directions (two different installation sites 2).

References

Borrelli L, Antronico L, Gullà G, Sorriso-Valvo GM (2014) Geology, geomorphology and dynamics of the 15 February 2010 Maierato landslide (Calabria, Italy). Geomorphology 208:50–73

Leva D, Nico G, Tarchi D, Fortuny-Guasch J, Sieber AJ (2003) Temporal analysis of a landslide by means of a ground-based SAR interferometer. IEEE Trans Geosci Remote Sens 41(4):745–752

Di Pasquale A, Corsetti M, Guccione P, Lugli A, Nicoletti M, Nico G, Zonno M (2013) Ground-based SAR interferometry as a supporting tool in natural and man-made disasters. In: Lasaponara R, Masini N, Biscione M (eds) Proceedings of the 33rd EARSel symposium, pp 173–186

Nico G, Leva D, Fortuny-Guasch J, Antonello G, Tarchi D (2005) Generation of digital terrain models with a ground-based SAR system. IEEE Trans Geosci Remote Sens 43(1):45–49